Radiometric profiling of temperature, water vapor and cloud liquid water using various inversion methods

Fredrick Solheim and John R. Godwin
Radiometrics Corporation, Boulder, Colorado

E. R. Westwater and Yong Han
Cooperative Institute for Research in Environmental Sciences, University of Colorado/NOAA, Boulder, Colorado

Stephen J. Keihm and Kenneth Marsh
Jet Propulsion Laboratory, Pasadena, California

Randolph Ware
University Corporation for Atmospheric Research, Boulder, Colorado

Abstract. We have developed a tunable temperature profiler based on a highly stable synthesizer that can observe at multiple frequencies on the shoulder of the 60 GHz atmospheric oxygen feature. We are developing a similar radiometer to obtain the vertical distribution of water vapor by making observations on the pressure broadened water vapor line from 22 to 29 GHz. Information on cloud liquid water profiles is also contained in these two wavebands. Various mathematical retrieval methods for temperature, water vapor, and cloud liquid water profiles were tested based on these radiometer designs. These include neural networking, Newtonian iteration of statistically retrieved profiles, and Bayesian "most probable" retrievals. Based on realistic radiometer errors and performance, very good retrieval capability is demonstrated. The performance of the various retrieval methods are presented and compared. Examples of profile retrievals are also presented. Data were not binned into seasons to reduce computer time; better retrieval results for all methods would be expected with binning.

1. Motivation for Radiometric Atmospheric Profiling

Radiosonde observations (RAOBs) are the fundamental method for atmospheric temperature, wind, and water vapor profiling, in spite of their inaccuracies, cost, sparse temporal sampling and logistical difficulties. A better technology has been sought for decades, but until now, no accurate continuous all weather technology has been demonstrated. Laser radars (LIDARS) and Fourier transform infrared spectrometers can profile temperature and water vapor, but not in the presence of cloud. Our highly stable frequency agile radiometric temperature and water vapor profilers give continuous unattended profile measurements. They also have the capability to profile cloud liquid water, a capability absent in RAOBs and all other systems except for *in situ* aircraft devices. Applications for this passive radiometric profiling include: weather forecasting and nowcasting; detection of aircraft icing and other aviation related meteorological hazards; determination of density profiles for artillery trajectory and sound propagation; refractivity profiles for radio ducting prediction; corrections to radio astronomy; satellite positioning and Global Positioning System (GPS) measurements; atmospheric radiation flux studies; estimation and predic-

tion of telecommunication link degradation; measurement of water vapor densities as they affect hygroscopic aerosols and smokes.

2. Microwave Profiling Methods

The microwave profiling methods discussed here make use of atmospheric radiation measurements in the 20 to 75 GHz region. The zenith path atmospheric absorption spectrum at sea level for a typical mid latitude atmosphere with a 1 km thick, 0.5 g/m^3 cloud in this frequency band is shown in Figure 1. The feature at 22.2 GHz is a water vapor resonance that is pressure broadened according to the pressure altitude of the water vapor distribution, while the feature at 60 GHz is an atmospheric oxygen resonance. The liquid water spectrum increases approximately with the second power of frequency in this region.
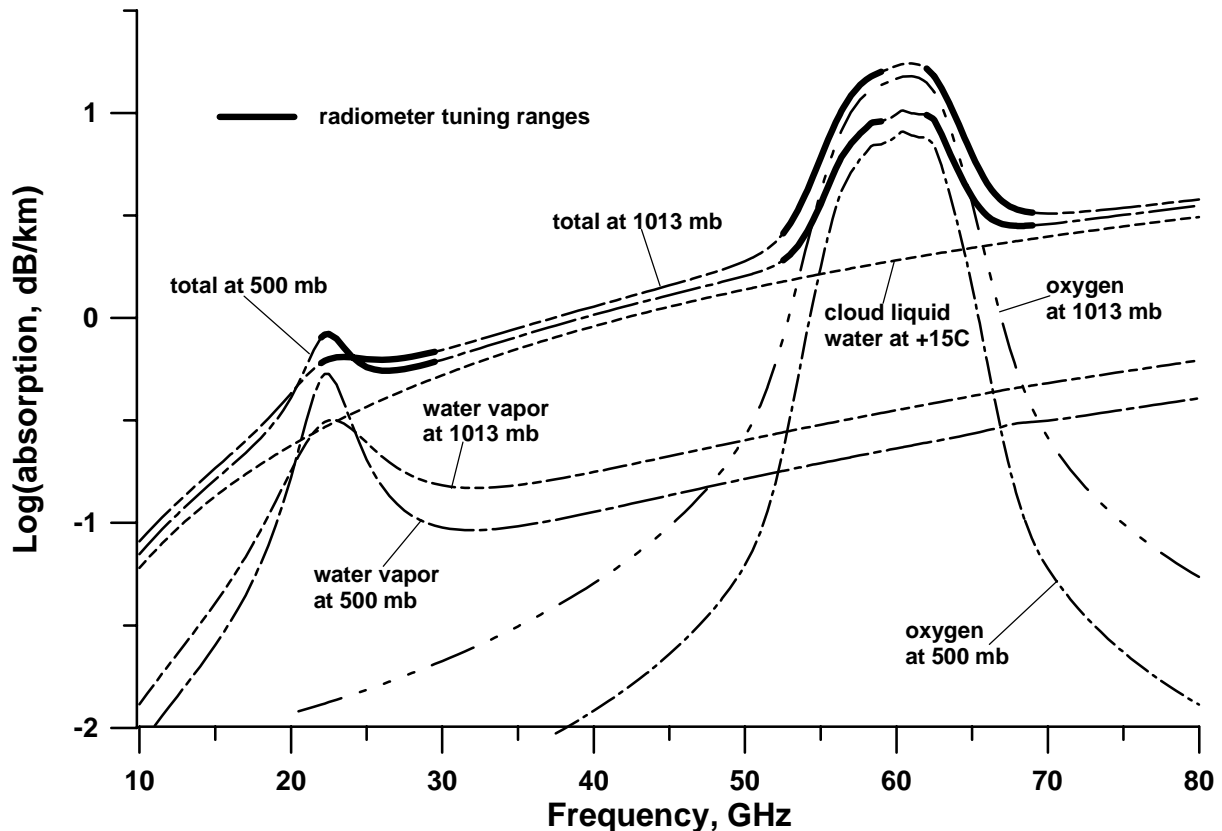

Figure 1. Contributions to atmospheric absorption by oxygen, water vapor, and cloud liquid water droplets. Radiometer tuning ranges are shown by the broadened traces. Absorption at two altitudes is shown to demonstrate pressure broadening.

Temperature profiles can be obtained by measuring the spectrum of radiation intensity, "brightness" spectrum, at points along the side of the oxygen feature at 60 GHz [*Westwater*, 1965]. By scanning outward from line center, where the opacity is so great that all signal originates from just above the antenna, onto the wing of the line, where the radiometer "sees" deeper into the atmosphere, one can obtain altitude information. Emission at any altitude is proportional to local temperature; thus the temperature profile can be retrieved. Either shoulder of this feature is suitable for retrieval of temperature profile information.

Water vapor profiles can be obtained by observing the intensity and shape of emission from pressure broadened water vapor lines. The water vapor line at 183 GHz is used for vapor profiling from satellites. The high opacity of this line hides the unknown emission emanating from the earth's surface, eliminating this error source but precluding profiling to low altitudes. The line at 22 GHz is too transparent for effective profiling from satellites but is suitable for ground based profiling. In this feature, the emission from water vapor is in a narrow line at high altitudes and is pressure broadened at low altitudes. The intensity of emission is proportional to vapor density. Scanning the spectral profile and mathematically inverting the observed data can therefore provide water vapor profiles.

Cloud liquid water profiles can be obtained by measuring the contribution of cloud liquid water to atmospheric spectral features of varying opacity. For instance, as described above, the atmospheric temperature profile can be obtained by scanning either side of the 60 GHz oxygen feature. Scanning from the line center outward onto either of the wings of the feature moves the observation deeper into the atmosphere, yielding altitude information on atmospheric temperature. Cloud liquid water, if present, contributes more to the 60 to 75 GHz high frequency side of this feature than to the 45 to 60 GHz low frequency side, thereby skewing the line shape. Therefore, scanning both sides of the line yields information on the temperature and cloud liquid profiles. There is also cloud liquid profile information in the combined 22 to 29 GHz and 52 to 59 GHz tuning bands.

3. Determination of Radiometer Frequencies with Maximum Information Content

As a first step in our analysis, the weighting functions defined by *Schroeder and Westwater* [1991] were numerically calculated for each 1992 Norman, Oklahoma, radiosonde using NOAA Environmental Technology Laboratory (ETL) weighting function software. Radiosonde data were separated into clear and cloudy sets. Weighting functions were calculated at 200 MHz intervals within the 20 to 29 (K-band) and 52 to 59 (V-band) GHz tuning wavebands and at 90, 30, and 14.5 degree elevation angles. This site was chosen because of its wide range of water vapor values and profile structures. Although optimum frequency ensembles are expected to differ for differing climatologies, we expect these differences to be slight.

The weighting function describes the change in signal at the radiometer antenna as a function of change in the vapor density profile:

$$W_{\rho_\upsilon}(s) = e^{-\tau(0,s)}\frac{\partial\alpha(s)}{\partial\rho_\upsilon}[T(s)] - T_{b0}e^{-\tau(s,\infty)} - \int_s^\infty T(s')\alpha e^{-\tau(s,s')}ds \qquad (1)$$

where ρ_υ is the density of water vapor in g/m^3, $\tau(s,s')$ is the opacity along a ray path from s to s', α is absorption in nepers, $T(s)$ is the physical temperature in K at coordinate s, and T_{b0} is the cosmic background temperature in K.

The next step is to determine the frequency ensemble that contains the maximum amount of independent information for retrieving the desired profile. Frequency selection was undertaken for the following purposes; (1) water vapor profiling using both the K and V bands, (2) temperature profiling using the V band only and using both the K and V bands, (3) cloud liquid water profiling

using the K band only and using both the K and V bands, (4) cloud liquid profiling using both sides of the 60 GHz oxygen feature, and (5) and cloud liquid profiling using both sides of the 60 GHz oxygen feature and the K band.
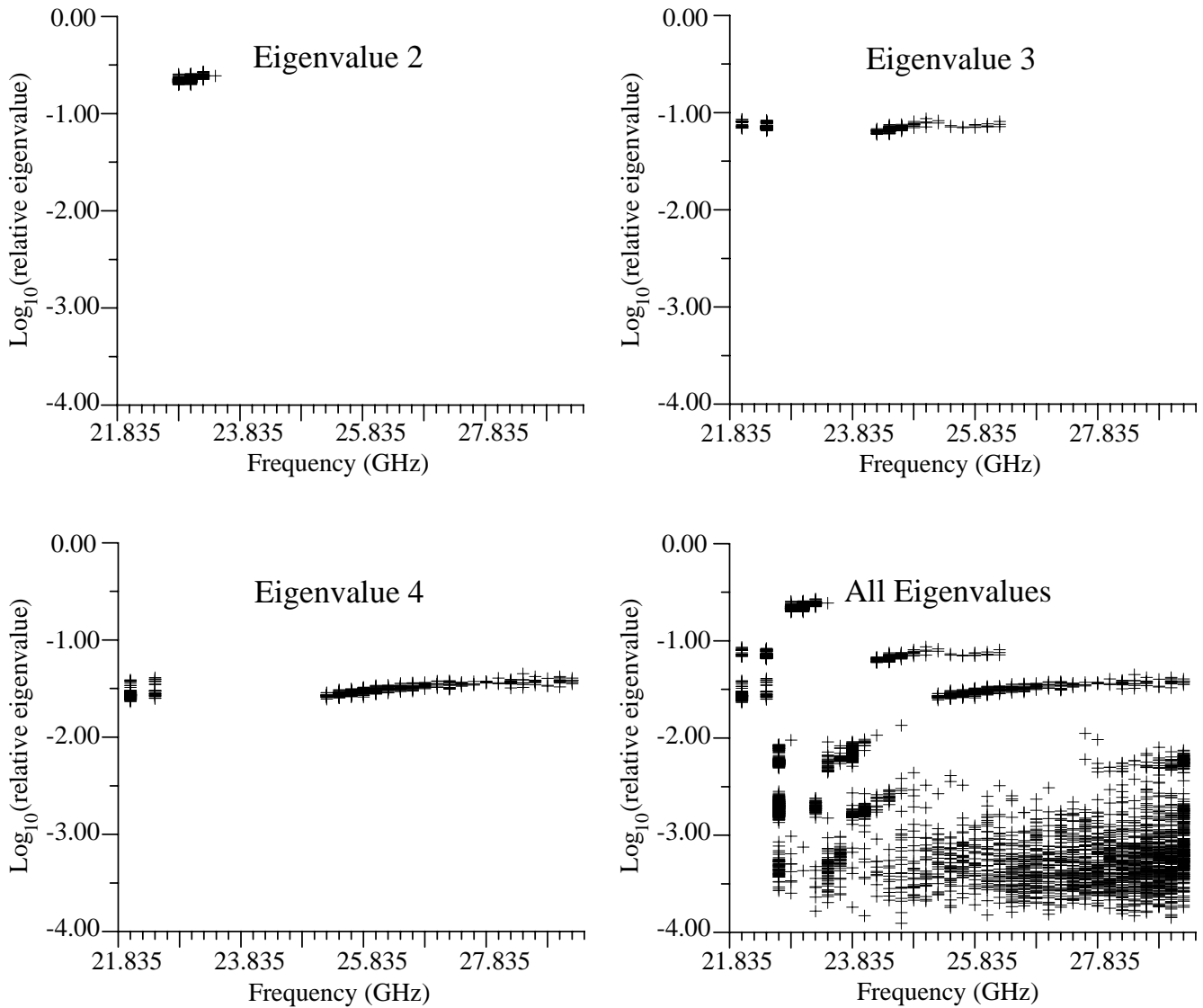

Figure 2. Water vapor eigenvalues calculated from RAOBS during clear conditions. The 22 to 29 GHz range is shown, and 22.235 GHz was pre-selected.

The frequency ranking was accomplished by pre-selecting the 22.235 GHz frequency since it contains the highest sensitivity to altitude. Each step of the algorithm involves adding a candidate frequency to the current frequency complement, forming the covariance matrix of the weighting functions and calculating its eigenvalues. If we consider the weighting functions at various altitudes to be components of a vector, then element c_{ij} of the covariance matrix is the inner (dot) product of w_i and w_j, where wi is the weighting function at frequency i. The eigenvalues of this covariance matrix contain information on the relative independence of the weighting functions. The additional eigenvalue that results from adding each remaining frequency to the current fre-

4

quency complement was summed by frequency for all radiosondes, and the frequency with the largest sum was included as the next most significant frequency in the frequency complement. Where the eigenfrequencies ranged across frequencies for the various soundings, a visual determination was made. The process was repeated to rank all of the frequencies. No additional information is obtained for the profile retrieval below a cut off that depends on radiometer brightness temperature accuracy.

Examples of scatter plots of water vapor eigenvalues are shown in Figure 2. Each cross represents an eigenvalue corresponding to the frequency being added to the frequency complement for one sounding. The eigenvalue corresponding to the pre-selected frequency is not shown. As more frequencies are selected, the chosen frequencies become less clustered. This is due to two factors; (1) the higher order eigenvalues represent higher frequency variations in the profiles and different frequencies will be optimal for detecting features which are localized at specific heights in the profile, and (2) high order eigenvalues contribute less additional information so it makes less difference which frequency is selected.

Table 1: Observation parameters for water vapor profiling as determined by eigenvalue analysis, ranked by information content. Frequencies for instrument error of 0.5 K are listed above the break in the data columns. Additional frequencies for 0.2 K error are listed below the break. Boldface are pre-selected frequencies.

22 to 29 GHz at 14.5o		22 to 29 GHz elevation scans				22 to 29 and 48 to 59 GHz at zenith		22 to 29 and 52 to 59 GHz elevation scans			
clear	cloud	clear		cloud		clear	cloud	clear		cloud	
22.235	**22.235**	**14.5**	**22.235**	**14.5**	**22.235**	**22.235**	**22.235**	**90.0**	**22.235**	**90.0**	**22.235**
23.035	23.035	14.5	23.035	14.5	23.035	23.035	23.035	14.5	23.835	14.5	23.635
22.435	22.035	14.5	22.435	14.5	22.035	22.435	22.435	30.0	22.635	30.0	22.635
26.235	27.035	14.5	26.235	14.5	27.035	48.220	48.220	14.5	29.235	14.5	29.235
23.835	23.835	14.5	23.835	14.5	23.835	24.035	24.035	30.0	22.035	30.0	22.035
22.635	22.635	14.5	22.635	30.0	22.635	53.330	52.850	90.0	52.850	90.0	51.760
						52.850	52.280	30.0	51.760	90.0	52.280
						52.280	51.760	90.0	52.280	90.0	52.850
						51.760	53.330	90.0	53.330	90.0	53.330
						51.250	51.250	14.5	23.235	14.5	24.635
						50.730	50.300	90.0	53.850	90.0	53.850
						50.300	50.730				
						49.780	53.850				

Examples of the frequency and elevation ranking for water vapor profiling are given in Table 1 in order of information content. These rankings should not be taken as absolute but as representative only, as they are based on Norman soundings and are therefore based on a specific climatology. The ranking will differ slightly for different sites. However, ground based weighting functions for the three atmospheric parameters considered herein are far from unique. Adjacent frequency and elevation choices are highly correlated and have essentially the same information content. Therefore, the optimal ensemble for Norman is probably optimal for a wide variance of climatologies. It should also be noted that there are many possible subsets of a large, highly dependent set of weighting functions that span the same space equally well. In particular, the choice of a different pre-selected frequency will result in different frequency complements. The

number of eigenvalues for a given cutoff will remain the same although marginal eigenvalues may drift slightly above and below the cutoff. Also, the choice of frequencies whose weighting functions are near zero will cause the frequency selection algorithm to produce unpredictable results.

4. Additional Profile Information

4.1. Ancillary Information on Cloud Base Altitude and Temperature

As demonstrated by *Han and Westwater* [1995], knowing cloud base altitude and temperature is a very strong constraint in retrieval of water vapor profiles. This is also a strong constraint in cloud liquid profile retrieval. Such constraints greatly improve profiles beyond levels indicated by the eigenvalues.

Cloud base temperature information can be obtained from a passive infrared pyrometer. Cloud base height can be obtained from a ceilometer. Knowing the temperature profile allows either hardware method to determine both cloud base temperature and altitude. It is therefore desirable to include one of these sensors with the radiometric instrument. The cloud base temperature is important for liquid profiling, and the infrared pyrometer would probably give a better measure of this temperature than determining it from a ceilometer and retrieved temperature profile. Use of pyrometer data was assumed in this study.

4.2. Radiosonde Statistics

All of the retrieval methods tested incorporated statistical information on the behavior of the three profile types that was obtained from a history of RAOBs. Although the eigenvalue analysis determines the number of independent measurements obtained from the radiometric spectral information, the ability to retrieve and resolve profiles by these methods is greatly enhanced by the statistical information from RAOBs.

5. Description of the Various Retrieval Methods

5.1. Newtonian Iteration Retrieval Method

Two methods developed at NOAA ETL were applied to retrieval of profiles and associated parameters from brightness temperature and in situ surface measurements. The first is described in this section and follows the methods described in *Han and Westwater* [1995]. The second method is described in the following section. For both methods, the simulated measurements included surface temperature, water vapor, pressure, and cloud base height as well as 12 zenith brightness temperatures. From these measurements, the following quantities were retrieved: water vapor profile, temperature profile, and integrated liquid. From the water vapor and temperature profiles, various integrated quantities can also be derived. Such quantities could include layer averaged water vapor, precipitable water vapor, geopotential height, and cloud thickness.

The relationship between the measurements, represented by the m-dimensional measurement vector **y**, and the quantities to be retrieved, represented by the n-dimensional profile vector **x**, may be expressed as

$$y = F(\mathbf{x}) \tag{2}$$

which is, in general, nonlinear. This expression may be viewed as a mapping of a profile vector in the n-dimensional profile space into the m-dimensional measurement space. The retrieval process solves the above equation and derives the profile **x** from the measurement **y**. It is important to note that in the problem encountered here, for a given measurements vector **y**, there are an infinite number of profile vectors that satisfy the above expression. Thus, a unique solution does not exist. Additional information about **x** is required to constrain the solution. One such information source is a statistical ensemble of a large number of historic radiosonde profiles. A technique that incorporates such a statistical constraint is the Newtonian iteration inversion method. The $(k+1)^{th}$ iteration solution can be expressed as:

$$\mathbf{x_{k+1}} = \mathbf{x_s} + \mathbf{S_k}\mathbf{K_k^T}(\mathbf{K_k}\mathbf{S_k}\mathbf{K_k^T} + \mathbf{S_e})^{-1}[\mathbf{y} - \mathbf{y_k} - \mathbf{K_k}(\mathbf{x_s} - \mathbf{x_k})] \tag{3}$$

where k = 0, 1, 2,…, $\mathbf{x_k}$ is the kth solution, **y** is the measurement vector with an error covariance matrix $\mathbf{S_e}$. $\mathbf{K_k}$ is calculated as:

$$\mathbf{K_k} = \partial\mathbf{F}/(\partial\mathbf{x})|_{x = x_k} \tag{4}$$

and contains weighting functions evaluated at the kth estimate $\mathbf{x_k}$ of **x**, and $\mathbf{y_k} = F(\mathbf{x_k})$. The statistical constraint is represented by x_s, and S_k is the mean and covariance matrix of the statistical ensemble. Implementation of this method is the following.

The profile vector has 99 elements. The first 49 elements are water vapor density at the levels $z_i = i \cdot 0.25$ km, where i = 0 to 48. The next 49 elements represent the temperature profile having the same vertical coordinates and the last element is the integrated liquid. The measurement vector has 14 elements including surface temperature and vapor density, and elements at each of the 12 specified frequencies.

The weighting functions associated with the brightness temperatures were calculated analytically using a NOAA ETL routine [*Schroeder and Westwater*, 1991 and 1992]. The weighting function associated with the integrated liquid is calculated using a perturbation method. In calculating the weighting functions, the integrated liquid is distributed moist adiabatically from the cloud base, that ithe liquid water is condensate from a saturated parcel being lofted adiabatically.

The statistical information may be used more efficiently by the classification of the statistical ensemble according to the cloud base heights, which can be identified from the relative humidity profiles. The statistical ensemble is divided into several sub-ensembles, each of which contains only the radiosonde profiles having the same cloud base height. For each sub-ensemble, $\mathbf{x_s}$ and $\mathbf{S_x}$ are calculated.

The retrieval process starts with the calculation of the initial profile $\mathbf{x_o}$. By using a regression method, the profile portion of the initial estimate $\mathbf{x_o}$ of **x** is obtained from surface water vapor and temperature measurements and the integrated liquid portion is obtained from the two brightness

temperatures at 23.835 and 29.235 GHz. The next step is to identify a set of $\{\mathbf{x}_s, \mathbf{S}_x\}_k$ by the cloud base height measurement. Then the iteration starts. For this experiment, the iteration is terminated at k=2.

5.2. Regression Retrieval Method

This method uses the traditional linear statistical inversion method summarized by *Westwater* [1993] and *Rodgers* [1976]. The independent vector y contains the 12 brightness temperatures, surface vapor density, and surface temperature. The dependent vector x contains the water vapor profile, temperature profile, and integrated liquid. The dependent vector is obtained linearly from the independent vector as:

$$\mathbf{x} = \mathbf{a} + b\mathbf{y} \tag{5}$$

where **a** and b are obtained from a statistical ensemble of radiosonde profiles using multivariate regression methods.

It is noted that the Newton iteration method explored by Han and Westwater yields slightly better results than the regression method due to the cloud base height data included in the iteration method. It is also noted that the cloud base height data utilized in the iteration method improves integrated liquid retrievals significantly in comparison with the regression method that does not use the cloud base height data.

5.3. Neural Networking

All neural networks were standard feed forward networks with input, hidden, and output layers with full connection between adjacent layers. A standard back propagation algorithm was used for training. Depending on the size of the data set, each RAOB was corrupted by Gaussian noise one to four times to decrease the sensitivity of the network to noise in the data. The limitation on data set size was due to available computer memory; the data sets ranged in size from 7,000 to 20,000 soundings. During training, the data were presented in randomized order approximately 5,000 times. For clear RAOBs, there were 39 input nodes: 36 brightness temperatures, surface temperature, vapor density and pressure, 39 hidden nodes and 47 output nodes representing the output profile every 0.1 km from 0 to 1 km and every 0.25 km from 1 to 10 km.

For cloudy conditions the cloud base information was represented by ones in a set of 47 height bins at the same heights as the output profile for a total of 86 input nodes. These networks had 86 hidden nodes and 47 output nodes. By adding a set of short cut connections directly from the input nodes to the output nodes we allowed the cloud base information to directly affect the corresponding output profile altitude. For cloud liquid, networks with only zenith brightness temperatures were used, including 62 input, 62 hidden and 47 output nodes. Their performance retrieving cloud liquid was equal to the networks with all 36 brightness temperatures, confirming our eigenvalue analysis that showed both data sets contained four independent measurements.

5.4. Bayesian Maximum Probability Method

The Bayesian algorithm was developed at the Jet Propulsion Laboratory (JPL) primarily for calibration of the wet tropospheric path delay during radio astronomy measurements such as the planned Gravitational Wave Search Experiment using the NASA Cassini spacecraft. Simulations at JPL demonstrated the superiority of the Bayesian inversion methods over linear regression for the precise monitoring of path delay variations using microwave radiometers [*Keihm and Marsh*, 1996].

The model based algorithm uses Bayes' rule to estimate the most probable value P of the state vector, **a** (e.g., vapor densities), given an observable vector, **y**, which consists of the brightness temperature measurements and surface meteorology data:

$$P(\mathbf{a}|\mathbf{y}) = P(\mathbf{y}|\mathbf{a})P(\mathbf{a})/P(\mathbf{y}) \tag{6}$$

where Gaussian statistics are assumed. The state vector, which defines the temperature and vapor density profiles over a vertical grid, is represented as a Karhunen-Loeve expansion, using eigenvectors derived from the *a priori* covariance of the state vector **a**. The state vector covariance matrix is calculated from a representative radiosonde data archive. An advantage of the Karhunen-Loeve representation is that it can reduce the number of independent unknowns. If the eigenvalues of the *a priori* covariance matrix are ordered by decreasing value, it often happens that only a fraction are significant; the rest represent noise. The inversion problem then reduces to estimating a smaller set of variables, the computational burden is reduced, and the accuracy of the inversion can increase if the elements of the state vector covariance matrix are not well determined from the radiosonde archive.

In practice, given a set of observables, the state vector is iterated, and the corresponding theoretical observables are computed, until the "most probable" (maximization of equation above) profile solution is obtained. In qualitative terms, the "most probable" profile solution is that which minimizes the residuals between measured and computed observables while best conforming to the constraints of the a priori statistics.

6. Performance Comparisons of the Retrieval Methods

Ten years of RAOBs including more than 6,000 soundings from Denver, Colorado, Norman and Oklahoma City, Oklahoma, and West Palm Beach, Florida, were used for training sets. These three sites were chosen because they represent a broad range of climatologies, and therefore a broad test of the retrieval methods. The subsequent three years of about 2,000 RAOB soundings were used as a test or verification set. Neural networking was applied to all three sites and all three profile types. The Bayesian method was applied to water vapor profiles for Denver clear cases. The Han and Westwater statistical regression and Newton iterative method were applied to Oklahoma all weather temperature and water vapor profiles. For simplicity, 12 frequencies to cover all types of profiles in clear and cloudy conditions were selected from the frequency complements (22.035, 22.235, 22.635, 23.835, 29.235, 51.760, 52.280, 54.400, 54.940, 56.020, 56.660, and 58.800 GHz) calculated from the eigenvalue analysis in Section 3. The radiative transfer model of NOAA [*Schroeder and Westwater*, 1992] was used to calculate brightness temperatures at the 12 frequencies and 3 elevation angles. These brightness temperatures plus surface

temperature, pressure and relative humidity, and up to two cloud base heights were the available observables for the retrieval methods. The root mean square (rms) gaussian errors used to corrupt the observables were 0.5 K for brightness temperatures and surface temperature, 3 mb for surface pressure, 1% for surface relative humidity and 100 m for cloud base data. We later determined that ceilometers are accurate to approximately 10 m.

Year round retrievals were utilized in all cases to conserve computing time. Had the retrievals been binned into seasons or months, we would expect some improvement in the rms retrieval errors and in the individual profiles.

The rms errors of temperature, water vapor, and liquid water profiles at Norman Oklahoma using various retrieval methods are shown in Figure 3. The standard deviation of each parameter as measured by the RAOBs is plotted. The rms error relative to this standard deviation indicates how much the profile is improved over an *a priori* mean profile. The ensemble average profile is also plotted to show fractional errors in the retrieved values. The retrievals were based on all season values; a better result (lower rms errors) would have been obtained if they had been binned into seasons or months.

For temperature retrievals, the performance of the various algorithms is comparable. Excellent retrieval performance is generally found for profiles without inversions and profiles with ground based inversions. Elevated inversions at the 0.5 km level or higher are generally smoothed in the algorithm solutions. Retrieval error rms values generally range from 1 to 2 K for the 1 to 5 km height interval simulations at the three sites. Relative to the inherent variability of temperature, the tested observational system typically provides a factor of 4 to 6 improvement in estimation accuracy over the 1 to 5 km range. An exception to this relative performance improvement is found in the West Palm Beach temperature retrievals above 3 km, which is due to the low inherent variability of temperatures at this site. The temperature retrieval performance degrades only slightly for cloudy conditions, compared to clear conditions. The most significant differences between cloudy and clear are found for the Oklahoma sites.

The various water vapor profiling algorithm performances were also comparable. However, comparisons of integrated vapor retrievals for the Denver clear cases revealed large reductions in retrieval error for the Bayesian algorithm relative to the statistical technique. The result suggests that the nonlinear iterative methods may produce significant improvements in vapor profile retrievals, relative to statistical algorithms, when retrieved vapor densities are averaged over coarser height resolution elements. This result warrants further evaluation.

For the high resolution grid spacing used in the present evaluation, vapor density retrieval accuracies better than 1 g/m^3 were generally obtained at all sites and altitudes. Drier sites (such as Denver) exhibit approximately 0.6 g/m^3 errors or less at all altitudes. Relative to the inherent variability at each site, the simulated retrievals showed approximately five times improvement for Denver and Norman and 2 to 3 times improvement for the West Palm Beach simulations over the 0 to 3 km height range where most of the water vapor resides. Only slight degradation in retrieval accuracy occurred for cloudy conditions. Elevated vertical structure on scales of 1 km is generally smoothed in water vapor profile retrievals, consistent with expectations based on the eigenvalue analysis.
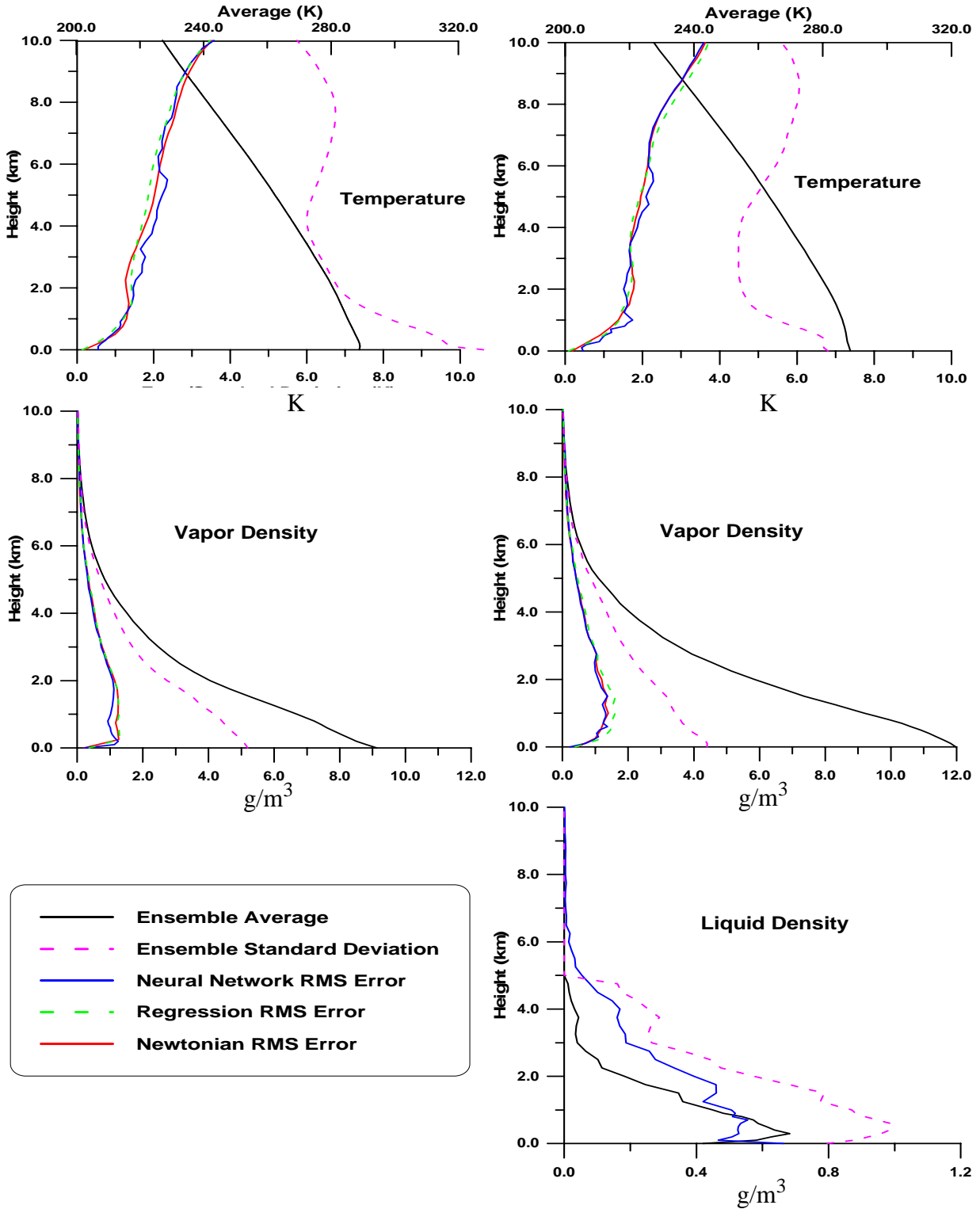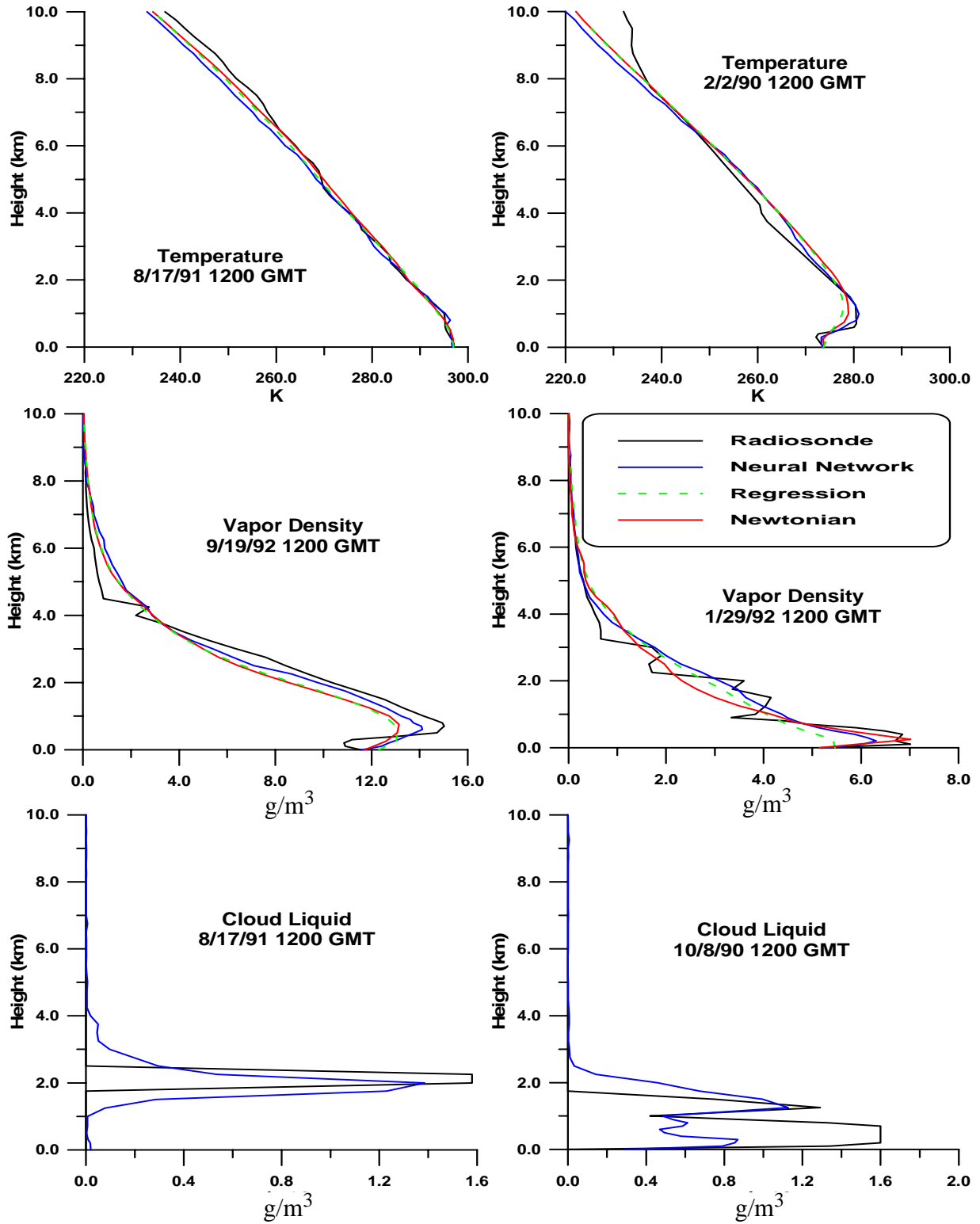
Figure 3. Examples of neural network, Newtonian, and statistical regression retrieved profiles for cloudy radiosonde data sets from Norman, Oklahoma. Typical "good" results are shown on the left, "poorer" results are shown on the right.

Figure 4. Examples of neural network, Newtonian, and statistical regression retrieved profiles for cloudy radiosonde data sets from Norman, Oklahoma. Typical "good" results are shown on the left, "poorer" results are shown on the right.
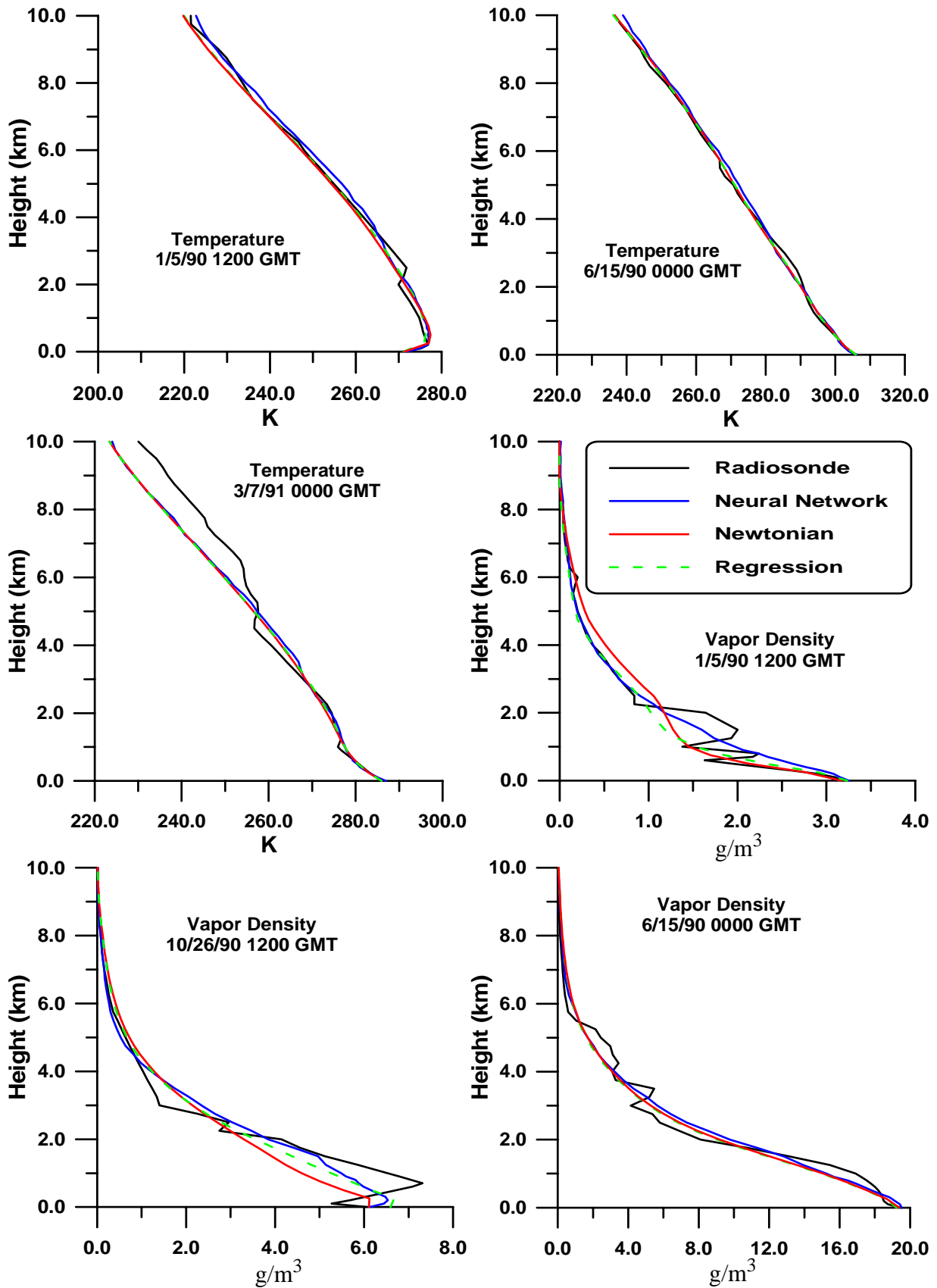
Figure 5. Examples of neural network, Newtonian, and statistical regression retrieved profiles for clear radiosonde data sets from Norman, Oklahoma.

The error of the neural network retrieved vapor density error at the surface improved from 0.4 g/m^3 to 0.3 g/m^3 for Oklahoma with surface relative humidity (RH) error improved from 2% to 1%. For a perfectly trained neural network we would expect about 0.15 to 0.20 g/m^3 error for 1% RH measurement error for Oklahoma City average surface absolute humidity of 5 to 6 g/m^3.

Cloud liquid profile improvements are not as dramatic in Figure 3, but this is due in part to the structure of clouds. Because we are determining the error at each altitude, slight altitude offsets in profile features between the actual and retrieved profiles can induce large errors when the retrieved parameter is changing rapidly with altitude. This is especially true of highly layered profiles such as cloud liquid water where the densities can change abruptly with altitude at the cloud margins. Additionally, the cloud bases were binned into 250 m intervals. The cloud margins therefore have an uncertainty of several hundred meters due to this deficiency in the retrieval method. The rms error evaluations are therefore not highly representative of ability to retrieve layered cloud structure. We have therefore included several individual profile retrievals in Figure 4 for a subjective demonstration and comparison of retrieval capability.

7. Conclusions

We conclude from our analysis that reasonably accurate atmospheric temperature, water vapor and liquid water profiles can be obtained from microwave radiometers and ceilometers data using a variety of mathematical retrieval methods. We are currently developing a profiling radiometer with these capabilities.

References

Han, Y. and E. Westwater, Remote sensing of tropospheric water vapor and cloud liquid water by integrated ground-based sensors, J. Atmospheric and Oceanic Technology, **12**, 1050-1059, 1995.

Keihm, S. J. and K. A. Marsh, Advanced algorithm and system development for Cassini radio science tropospheric calibration, Progress Report for the JPL Telecommunications and Data Acquisition Program, in preparation, 1997.

Rodgers, C. D., Retrieval of Atmospheric Temperature and Composition from Remote Measurement of Thermal Radiation, Rev. Geophys. & Space Phys., **124**, 609-624, 1976.

Schroeder, J., and E. Westwater, User's guide to microwave radiative transfer software, NOAA Technical Memorandum ERL WPL-213, NOAA Wave Propagation Lab., Boulder, Colo., 1991.

Schroeder, J., and E. Westwater, Guide to microwave weighting function calculations, NOAA Technical Memorandum ERL WPL-225, NOAA Wave Propagation Lab., Boulder, Colo., 1992.

Westwater, E. R., Ground-based Microwave Remote Sensing of Meteorological Variables, Chapter 4 in Atmospheric Remote Sensing by Microwave Radiometry, M. Janssen, editor, J. Wiley & Sons, NY, 145-213, 1993.

Westwater, E., Ground-based passive probing using the microwave spectrum of oxygen, Radio

Science, **9D**, 1965.

_____

J. Godwin and F. Solheim, Radiometrics Corporation, 2898 30th Street, Boulder, CO 80301-1212. (303) 449-9192 fax: (303) 786-9343, email: solheim@radiometrics.com

Y. Han and E. Westwater, NOAA ETL, 325 Broadway, Boulder, CO 80303, (303) 497-7019, email: yhan@etl.noaa.gov

S. Keihm and K. Marsh, Jet Propulsion Laboratory, 4800 Oak Grove Drive, Pasadena, CA 91109-8099, (818) 354-3656, email: stephen.j.keihm@ccmail.jpl.nasa.gov

R. Ware, University Corporation for Atmospheric Research, POB 3000, Boulder, CO 80307, (303) 497-8005, email: ware@ucar.edu.